International Journal of Advanced Materials and Production, Vol.1, No. 1, December, 2016

First-principles calculations of $CaMg_2$ Alloy Phase to predict its Electronic and Elastic Properties

Jia Fu [1,a*], Weihui Lin [2,b] and Zhongren Chen [3,c]

[1] Department of Material, Southern University of Science and Technology, Shenzhen, China
[2] School of Mechanics College, Taiyuan University of Technology, Taiyuan, China
[3] Department of Chemistry, Southern University of Science and Technology, Shenzhen, China

Abstract. The influencing effect of pressure on structural, elastic and electronic properties of $CaMg_2$ Laves phase is mainly investigated. The optimized structural parameters at zero pressure are a=b=6.250Å, c=10.101Å, which has good agreement with the experimental and theoretical values. The elastic constants are calculated, and then the bulk modulus, shear modulus, Young's modulus, Poisson's ratio and anisotropy factor are determined. The results show that the applied pressure is beneficial to the elastic properties of $CaMg_2$. The analysis of electronic density of states (DOS) and Mulliken electron population reveal the bonding characteristics in $CaMg_2$ crystal. Finally, the Debye temperatures under different pressures are obtained from the average sound velocity.

Keywords: *$CaMg_2$; elastic constants; Young's modulus; DOS analysis; Debye temperature;*

I. Introduction

As the good strength to weight ratio of common structural materials, magnesium (Mg) alloys have received much attention [1,2]. Magnesium alloys as low density, high specific strength, good stiffness and strength-weight ratio are widely used in aerospace industry, automobile industry, 3D printing and other fields [2, 3]. Therefore, much work has been focused on improving the mechanical properties of Magnesium alloys. Experimental investigations show that Magnesium alloys can be significantly improved by adding rare-earth (RE) elements [4] and Ca element [5]. The Laves phases in Mg alloys have been gradually focused because of their excellent physical and chemical properties [6-12].

In the past few years, some experiments have been carried out to study Laves phases in Mg-Al-Ca alloys , such as $CaAl_2$(C15), $CaMg_2$(C14), $(Mg,Ca)Al_2$(C14) and $Ca(Mg,Al)_2$(C36) [13,14]. However, the application of magnesium alloys in the modern industry currently is still limited due to their restricted mechanical properties [5,15]. Under this background, the binary system of Mg-Ca is regarded as one of the most promising candidates for biodegradable implant applications due to its good biocompatibility, no toxicity and appreciable corrosion resistance [17]. $CaMg_2$ Laves phase is a typical phase in Mg-Ca, Mg-Al-Ca and Mg-Zn-Ca alloy systems. In the Mg-Zn binary alloys, the grain can be significantly refined by adding the inexpensive element Ca, which can increase the density of aging precipitates $MgZn_2$ phase, thereby improving the mechanical properties of the alloy [5].

Mg-Ca alloy exhibits excellent oxidation-resistance and burning-resistance [16], and it is also regarded as one of the most promising alloy due to its appreciable corrosion resistance [17]. $CaMg_2$ Laves phase as its excellent physical and chemical properties is a typical phase in Mg-Y-Ni [18] and Mg-Al-Ca alloy [14]. Yu et al. [19] investigated the electronic structure and elastic properties of the binary AB_2 type Laves phase in Mg-Al-Ca alloys, indicating that the $CaMg_2$ phase has a strong alloying ability as well as a strong structural stability. Ca is an important alloying element of Mg, and is also a lower cost and weight element than rare-earth elements. Elastic constants and electronic structure of $CaMg_2$ alloy are studied by Tang et al.[3], indicating that the stability of C14 $CaMg_2$ Laves phase alloy is strong. Zhou et al. [17] has investigated the phase stability and electronic structure of an Mg-Ca system, showing that $CaMg_2$ Laves phase is ductile with a structural stability. Mao et al.[20] studied the structural, elastic and electronic properties of AB_2 type intermetallics in Mg-Zn-Ca-Cu alloy from First-principles calculations. However, there is no report about the experimental

Manuscript received August 16, 2016; revised October 8, 2016; accepted November 1, 2016.

*corresponding author, Email: fuj@sustc.edu.cn

values of Debye temperature and theoretical study of the pressure effect on structural, elastic and electronic properties of $CaMg_2$ Laves phase.

In this work, the first-principles calculations are used to investigate the structural parameters, the anisotropic elasticity, elastic and electronic properties of the C14 $CaMg_2$ Laves phase under pressure. Moreover, the density of state (DOS) under different pressure is analysed to insight into the bonding characteristics of $CaMg_2$, and then reveals the underlying structural stability mechanism of $CaMg_2$ Laves phase. The results are compared with the available experimental and theoretical values.The current work can act as a theoretical prediction and provides mechanical parameters of $CaMg_2$ alloy.

II. Theoretical principle and calculation algorithm

A. Description of elastic constants algorithm and Young's modulus calculation

A multi-particle electronic structure satisfies the Schrödinger equation. Generally, Hamiltonian contains kinetic energy, Coulomb potential energy between electrons and the external potential, which is described as:

$$H=\sum_i -\frac{\mathrm{h}^2}{2m}\nabla_i^2+\sum_{i,j}{}'\frac{e_1^2}{\left|\mathrm{r}_i-\mathrm{r}_j\right|}+\sum_i V_i\left(\mathrm{r}\right) \tag{1}$$

Where, $V_i(r)$ is an external potential; r_i and r_j are the nucleus position vectors; while mε and m stand respectively for the mass of nuclei and electrons. h is the reduced Planck constant.

Kohn-Sham equation as an approximation to simplify Schrödinger equation is described as [21]:

$$\begin{cases}\left[-\frac{\mathrm{h}}{2m}\nabla^2+V_{eff}\left(\mathrm{r}\right)\right]\varphi_i\left(\mathrm{r}\right)=\varepsilon_i\varphi_i\left(\mathrm{r}\right)\\ V_{eff}\left(\mathrm{r}\right)=V\left(\mathrm{r}\right)+V_{ee}\left(\mathrm{r}\right)+V_{ex}\left(\mathrm{r}\right)\\ V_{xe}\left(\mathrm{r}\right)=\frac{\delta E_{xe}[\rho]}{\delta\left(\mathrm{r}\right)}\\ \rho\left(\mathrm{r}\right)=\sum_i\left|\phi_i\left(\mathrm{r}\right)\right|^2\end{cases} \tag{2}$$

Where, $V_{xe}\left(\mathrm{r}\right)$ is an exchange-correlation potential; $\rho\left(\mathrm{r}\right)$ is the electron density. Equation (2) includes not only the nucleus and electron kinetic energy term but also term of nucleus- nucleus and electron-electron interactions [21]. The electron density is optimised and elastic constants are obtained.

Elastic constants are often used to characterize resist deformation capacity to an externally applied stress. For hexagonal structure, there are 5 independent elastic constants (C_{11}, C_{12}, C_{13}, C_{33} and C_{44}, since $C_{66}=(C_{11}-C_{12})/2$), mechanical stability condition and Voigt/ Reuss bounds of *B* and *G* are[22]:

$$C_{11}>0;C_{11}-C_{12}>0;C_{44}>0;(C_{11}+C_{12})C_{33}-2C_{13}^2>0 \tag{3}$$

$$B_V=\frac{2}{9}(C_{11}+C_{12}+\frac{1}{2}C_{33}+2C_{13}) \tag{4}$$

$$G_V=\frac{1}{30}(7C_{11}-5C_{12}+12C_{44}+2C_{33}-4C_{13}) \tag{5}$$

$$B_R=\frac{(C_{11}+C_{12})-2C_{13}^2}{C_{11}+C_{12}+2C_{33}-4C_{13}} \tag{6}$$

$$G_R=\frac{5}{2}\left\{\frac{[(C_{11}+C_{12})C_{33}-2C_{13}^2]C_{44}C_{66}}{3B_VC_{44}C_{66}+[(C_{11}+C_{12})C_{33}-2C_{13}^2](C_{44}+C_{66})}\right\} \tag{7}$$

Then homogenized elastic properties of polycrystals can be derived. Shear and bulk moduli are obtained by means of Voigt and Reuss bounds, which are based on the C_{ij} calculated. Then the Voigt-Reuss-Hill average and Young's modulus can be determined from shear/bulk modulus [22, 23].

Defining $\sigma_{11}=E_1\varepsilon_{11}$, $\sigma_{22}=E_2\varepsilon_{22}$ and $\sigma_{22}=E_2\varepsilon_{22}$, the formula of axial modulus in *x*, *y*, *z*-direction E_3 is shown as [24]:

$$E_1=E_2=\left(c_{11}-c_{12}\right)\left[1+\left(c_{12}c_{33}-c_{13}^2\right)/\left(c_{11}c_{33}-c_{13}^2\right)\right] \tag{1}$$

$$E_3=c_{33}-2c_{13}^2/\left(c_{11}+c_{12}\right) \tag{2}$$

Thus axial moduli in *x*, *y*, *z*-direction based on elastic constants calculated can be obtained. Therefore, Then homogenized Young's modulus *E*, Poisson's ratio and anisotropy factor *A* are obtained according to the following formula [25]:

$$E=\frac{9BG}{3B+G} \tag{8}$$

$$\nu=\frac{3B-2G}{2(3B+G)} \tag{9}$$

$$A=\frac{C_{11}-C_{12}}{2C_{44}} \tag{10}$$

Based on C_{ij}, Debye temperatures can be estimated by the some sound velocity equations [26]:

$$\Theta_D=\frac{h}{k_B}\left[\frac{3n}{4\pi}\left(\frac{N_A\rho}{M}\right)\right]^{1/3}V_m \tag{8}$$

$$V_m=\left[\frac{1}{3}\left(\frac{2}{V_s^3}+\frac{1}{V_l^3}\right)\right]^{-1/3} \tag{9}$$

$$V_s=\sqrt{\frac{G}{\rho}} \tag{10}$$

$$V_l=\sqrt{\left(B+\frac{4}{3}G\right)\frac{1}{\rho}} \tag{11}$$

Where Θ_D is Debye temperature; *h* and k_B are the Planck and Boltzmann constant; *n* the total number of atoms; ρ is density; N_A the Avogadro number; *M* the molecular weight per formula; V_m the average sound velocity; V_s the transverse sound velocity and V_l the longitudinal sound velocity.

B. Modeling of CaMg2 and computational method

Cambridge sequential total energy package (CASTEP), and first-principles plane wave pseudo-potential method based on density functional theory (DFT) [27] is used for the calculations. The exchange correlation potential is considered by the generalized gradient approximation (GGA) in the scheme of Perdew-Burke-Eruzerhof (PBE) [28].

Fig.1 shows $CaMg_2$ crystal of hexagonal structure with a space group $P6_3/mmc$ (No.194). There are 12 atoms in the unit cell, including 4 Ca atoms and 8 Mg atoms. Ca atoms are located on *4f* sites and Mg atoms *2a*, *6f* sites. Pseudo atomic calculations are performed for Mg $2p^6\ 3s^2$ and Ca $3s^2\ 3p^6\ 4s^2$.

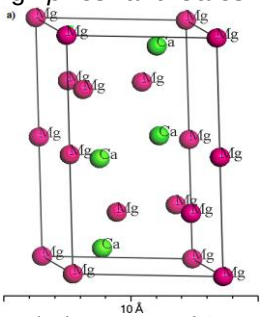

Figure.1 Final arameters of $CaMg_2$ crystal

As shown in Fig.1, crystal lattice is as: $a=b$=6.250Å, c=10.101Å, $\alpha=\beta$=90°, γ=120°. Geometry optimization with optimizing cell was firstly performed to determine the equilibrium structural parameters. The total energy as a function of the cell volume was fitted by Birch-Murnahan equation of state (EOS) [29,30], the obtained equilibrium volume corresponding to minus total energy is 341.732Å^3.

DFT calculation and initial conditions are as: the exchange-correlation function is GGA; Cutoff energy of the plane waves for ultrasoft pseudopotentials is 400*eV,* which is sufficient to fully converge. Brillouin zone is sampled with a mesh of 12×12×8 generated by Monkhorst-Pack method [31]. Geometry optimization is carried out with optimizing cell by the scheme of the Brodyden-Fletcher-Goldfarb-Shanno (BFGS) [32] minimization until the self-consistent convergence of the total energy value is 5.0×10^{-6}eV/atom, the force on all atoms is less than 0.001eV/nm, and the pressure region is 0～60*GPa*. The elastic constants of $CaMg_2$ are obtained by the stress-strain method [33,34].

III. Results and discussion

C. Structural parameters and elastic constants

The calculated equilibrium lattice parameters *a*, *c* and *c/a*, elastic constants C_{ij} and bulk modulus B_0 are listed in Tab.1.

Table I. The structural parameters (a0, c0, c0/a0, V0), elastic constants and bulk modulus B0 of CaMg2 phase at 0GPa.

a) Lattice parameters

	a_0(Å)	c_0(Å)	c_0/a_0	V_0(Å^3)
This work	6.250	10.101	1.616	341.732
Cal.[19]	6.240	10.140	1.625	342.200
Cal.[3]	6.232	10.093	1.620	339.740
Exp.[18]	6.220	10.100	1.624	341.081

b) Elastic constants

	C_{11}	C_{12},	C_{13}	C_{33}	C_{44}
This work	55.70	18.05	15.26	58.39	16.95
Cal.[20]	51.43	22.31	14.73	58.51	14.32
Cal.[4]	62.95	15.27	13.64	65.20	17.77

From Table 1 a), it is evident that the equilibrium lattice parameters from the present calculation match well with available experimental and theoretical values, it is indicated that the present model is reliable. It can be clearly seen that the volume of the unit cell is becoming smaller and smaller with the increasing pressure, which implies that the distance between atoms is getting smaller and smaller. As the pressure rises, the change of distance between atoms is smaller because of the repulsion force between atoms. The smaller the distance is, the stronger the repulsion force is.

The calculated elastic constants of $CaMg_2$ at zero pressure are tabulated in Table I b), and the calculated results in this work are in good agreement with previous theoretical values. Moreover, elastic constants satisfy the mechanical stability condition, which demonstrates the mechanical stability of $CaMg_2$ phase. The fairly good agreement with experimental and theoretical values in references shows that the present calculations are highly reliable.

Variations of the relative change of lattice parameters a/a_0, c/c_0 and the relative change of unit cell volume V/V_0 with increase of pressure are plotted in Fig.2.

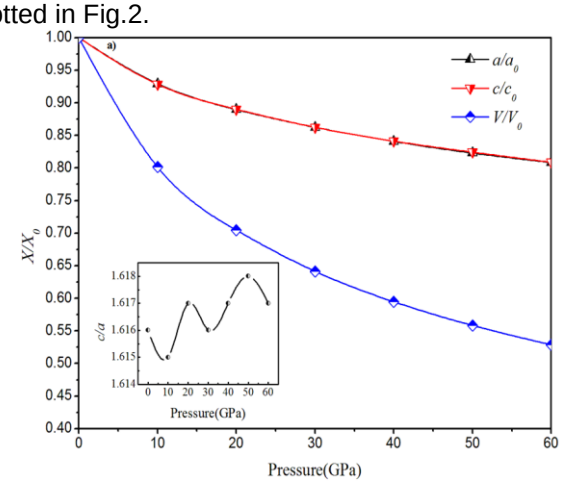

Figure.2 Relative change of a/a_0, c/c_0 and V/V_0

As shown in Fig.2, it can be seen that $CaMg_2$ has not undergone a phase transition according to the smooth variation of a/a_0, c/c_0 and V/V_0 with the increase of pressure. Moreover, it shows that the changes of the lattice parameter *a* and the

parameter *c* are so close to each other and almost equal throughout the whole pressure range with intervals of 10GPa, indicating that the elastic anisotropy of $CaMg_2$ is weak. The compressive ability of $CaMg_2$ crystal under pressure becomes difficult because of the strong repulsion force, which is consistent with the variation trend of the V/V_0 curve. The axial ratio *c/a* changes quite little (only 0.003) with increase of pressure, from the minimum 1.615 at 10GPa to the maximum 1.618 at 50GPa, and the axial ratio *c/a* decreases above 50GPa. This *c/a* variation of $CaMg_2$ is in good agreement with that of $MgZn_2$ phase reported by Liu et al. [35]. The values of ratio *c/a* under different pressures are all close to the ideal value 1.633 for typical hexagonal close-packed phase within an error less than 1.1%.

Fig. 3 gives us an intuitive variation of elastic constants C_{ij} with increasing pressure. The inset of Fig.3 is *B*, *G* and *E* as a function of the applied pressure.

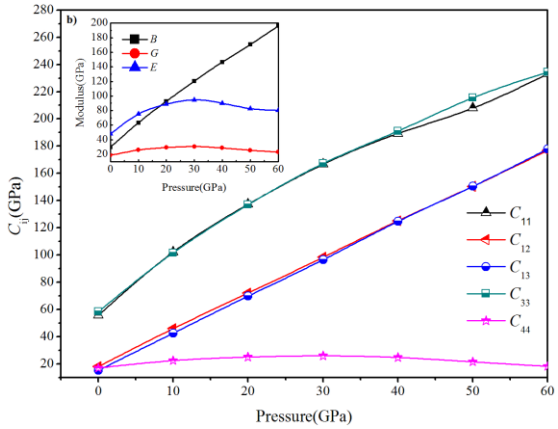

b) Elastic constants C_{ij}

Figure.3 Parameters under pressure of 0- 60Gpa

As in Fig. 3, we can conclude that C_{11} and C_{33} are more sensitive to the change of applied pressure than C_{12} and C_{13}, which can be attributed to the differences of the compressibility at different directions. Besides, the applied pressure has less effect on C_{44} and *G*, which have changed little with increasing pressure. Moreover, the elastic constants C_{11}, C_{12}, C_{13}, C_{33}, bulk modulus *B* and Young's modulus *E* show the increasing tendency with the increase of pressures. We can conclude that the applied pressure has a larger effect on C_{11}, C_{12}, C_{13}, C_{33}, *B*, *E* than on C_{44} and *G*.

D. Prediction of elastic moduli of $CaMg_2$ ploycrystals

Poisson' ratio is also a measure of the stability of the crystal against shear deformation, and a larger value is usually associated with a better plasticity [30]. Besides, the ratio of shear modulus to bulk modulus *G/B* of polycrystalline phase introduced by Pugh is used to predicate the brittle and ductile behavior of materials [36]. Evidently, a high *G/B* value is associated with brittleness while a low value associated with ductility.

The bulk modulus *B* of a material is usually used to be a measure of resist deformation capacity upon applied pressure [33]. The larger the value of *B* is, the stronger capacity of the resist deformation is [20]. Similarly, the shear modulus *G* is often employed to a measure of resist reversible deformation by shear stress [36]. The larger the value is, the stronger the capacity of resist shear deformation is.

To investigate the effect of the applied pressure on structural properties of $CaMg_2$, The changes of Poisson's ratio and *G/B* with increasing pressure are plotted in Fig.3

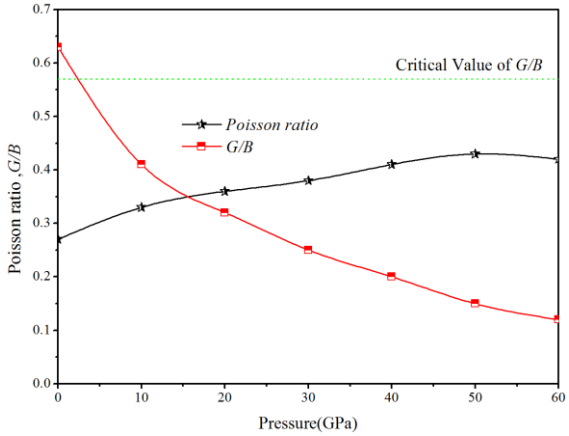

Figure.3 The pressure independence of Poisson's ratio and the *G/B* ratio of $CaMg_2$

As shown in Fig.3, the *G/B* ratio decreases with the increasing pressure. Poisson's ratio at 0*GPa* is 0.27, showing $CaMg_2$ is with predominantly central interatomic forces. The critical value which separates brittleness and ductility is about 0.57 in the horizontal dotted line. Evidently, the *G/B* ratio within region of 0～4*GPa* is higher than critical value 0.57 at 4*GPa*, which implies that $CaMg_2$ phase show a little brittle at 0*GPa* (*G/B* =0.63) and turn to be a ductile behaviour after critical value. It is indicated that $CaMg_2$ shows slight brittleness under 0～4*GPa* and good ductility under 4～60*GPa*.

The derived relative parameters of $CaMg_2$ under different pressure are listed in Table II.

Table II. The derived bulk modulus B, shear modulus G, Young's modulus E, Poisson's ratio μ and the ratio G/B and elastic anisotropy A of CaMg2 under different pressure.

Pressure	*B*	*G*	*E*	μ	*G/B*	*A*
0 GPa	29.70	18.48	47.89	0.27	0.63	1.11
0 Ref. [19]	31.06	18.99	55.74	0.20	0.61	0.79
0 Ref. [20]	29.43	15.72	40.04	0.27	0.53	0.98
10 GPa	63.12	25.89	75.02	0.33	0.41	1.25
20 GPa	92.71	29.34	88.66	0.36	0.32	1.29
30 GPa	120.46	30.57	94.62	0.38	0.25	1.32
40 GPa	146.52	28.79	90.18	0.41	0.20	1.30
50 GPa	170.52	25.71	82.72	0.43	0.15	1.33
60 GPa	196.23	23.00	80.20	0.42	0.12	1.55

From Table II, it can be found that *E* and *G* are satisfied with the relation $G=E/[2(1+\mu)]$. Moreover, Poisson's ratio increases with increasing the applied

pressure, which indicates that the applied pressure is beneficial to the plasticity of $CaMg_2$ phase. It is worthwhile to note that the *G/B* ratio is 0.63 (higher than 0.57) at 0GPa, which implies that $CaMg_2$ phase is a little brittle at zero pressure. When the pressure is above 10GPa, the *G/B* ratio is lower than 0.57, indicating a ductile behavior of $CaMg_2$. The result from *G/B* ratio is in good agreement with that from Poisson's ratio. Both of them reveal the ductility of $CaMg_2$ Laves phase under pressure.

E. Analysis of the density of state (DOS) and bonding characteristics

Structural stability of intermetallic compound is associated with its bonding electronic orbits. For covalent bond, it depends on the depth and width of band gap near Fermi level, while ionic bond is determined by the charge transfer between atoms. The density of state (DOS) under different pressure was calculated to have a further insight into the bonding characteristics of $CaMg_2$, and then reveals the underlying structural stability mechanism of $CaMg_2$ Laves phase.

The total and partial DOS of $CaMg_2$ phase near Fermi level under 0GPa, 20GPa, 40GPa and 60GPa are shown in Fig.4, respectively.

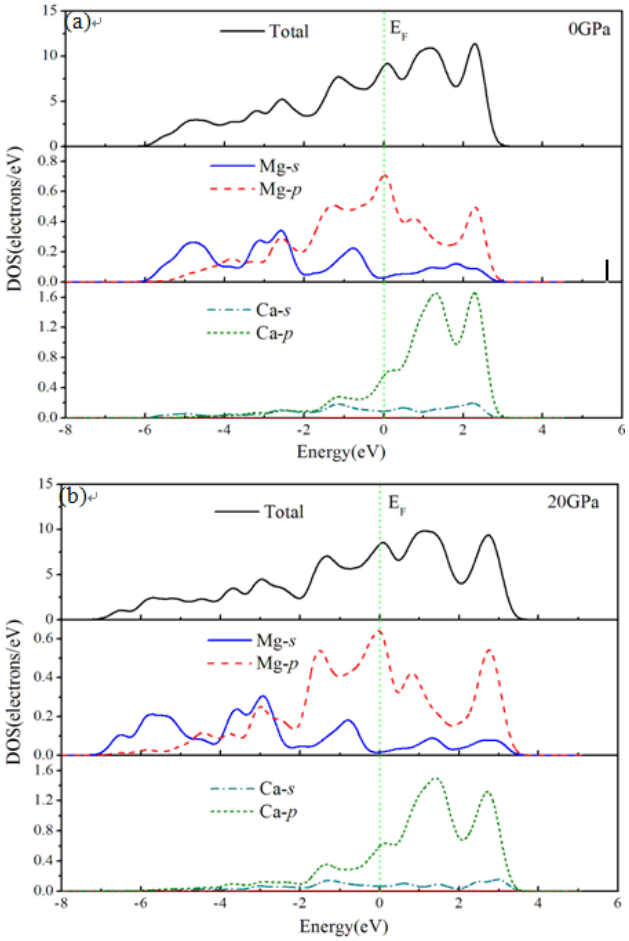

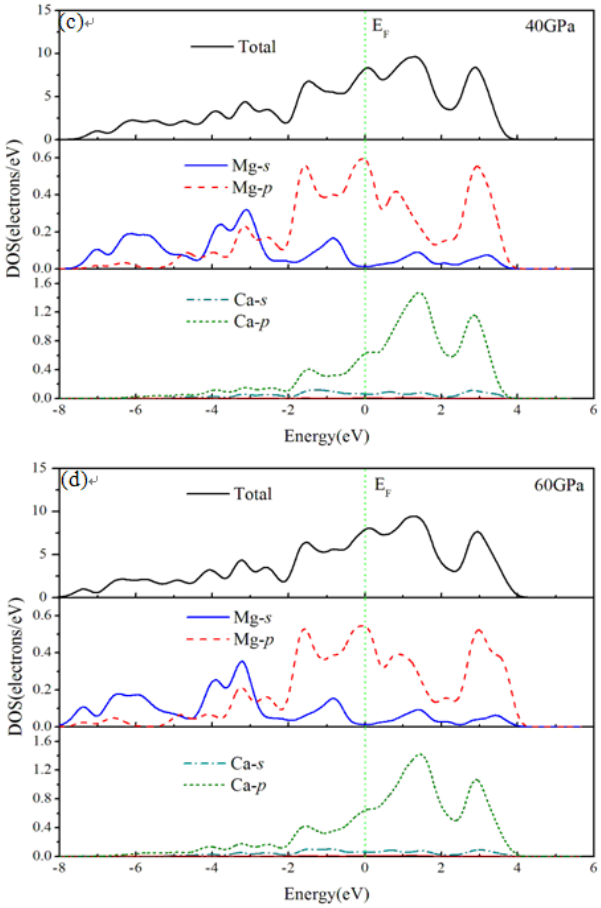

a) at 0*GPa*; b) at 20*GPa*; c) at 40*GPa*; d) at 60*GPa*.

Figure.4 The total and partial density of states (DOS) of CaMg2

As is shown in Fig.4, the total DOS of $CaMg_2$ is mainly made up of the *s, p* states of Mg atoms below Fermi level and the *s*, *p* states of Ca atoms above Fermi level. It is evident that the total DOS of $CaMg_2$ decreases with elevated pressure, which implies that applied pressure is of benefit to the stability of $CaMg_2$. Moreover, by the DOS analysis in Fig.4, $CaMg_2$ is characterised to have the metallic behaviour as there is no energy gap near the Fermi level, which is consistent with the results reported in previous literatures [3,17,19,20].

From Fig.4 b) to Fig.4 d), the shifting of Mg *s* and *p* orbits from higher to lower energy region is discovered and is observed towards the low energy region. Moreover, with increasing pressure, the Ca *s* and *p* orbits present a slight broadening and a decrease of intensity, which indicates that the hybridization of Mg *s, p* and Ca *s, p* orbits is becoming stronger. It is worthwhile to note that the DOS of $CaMg_2$ at 40 and 60GPa are almost the same, and that the applied pressure has a little effect on the DOS when the pressure is above 40*GPa*.

The DOS result is in good agreement with the references [3, 20]. The total and partial DOS near Fermi level may be attributed to the variations of the spacing between atoms as well as the overlap of

wave functions under compression.

F. Analysis of Mulliken electron population and Debye temperature

The Mulliken electron population has been performed to consider the ionic bond feature of $CaMg_2$ phase. As the thermodynamic properties of solids at high pressures and high temperature is also concerned, the Debye temperature as a fundamental parameter is related to lots of physical properties of solids, such as specific heat, elastic constants and melting temperature. At low temperatures the vibrational excitations arise solely from acoustic vibrations. Therefore, the Debye temperature obtained from elastic constants is the same as that determined by specific heat measurements.

Table III shows the calculated results of Mulliken electron population and dependent parameters (eg. the density ρ, the transverse sound velocity V_s, the longitudinal sound velocity V_l, the average sound velocity V_m and the Debye temperature Θ_D) of $CaMg_2$ under pressure of 0GPa～60GPa with an interval of 10 GPa.

Table III. a) Mulliken electron population of pressure;

Pressure	Species	s	p	d	Total	Charge (e)
0GPa	Ca	2.44	6.00	0.66	9.10	0.90
	Mg (I)	0.92	7.45	0.00	8.37	-0.37
	Mg (II)	0.93	7.55	0.00	8.48	-0.48
30GPa	Ca	2.32	5.98	1.00	9.30	0.70
	Mg (I)	0.89	7.31	0.00	8.20	-0.20
	Mg (II)	0.90	7.50	0.00	8.40	-0.40
60GPa	Ca	2.27	5.96	1.25	9.48	0.52
	Mg (I)	0.93	7.09	0.00	8.02	-0.02
	Mg (II)	0.95	7.39	0.00	8.34	-0.34

b) Pressure dependence of parameter ρ, Vs, V_l, V_m and Θ_D

Pressure (GPa)	ρ (kg/m^3)	V_s (m/s)	V_l (m/s)	V_m (m/s)	Θ_D (K)
0	1.724×10^3	3277.83	5614.24	3635.41	348.70
10	2.150×10^3	3470.14	6249.48	3865.02	399.02
20	2.447×10^3	3462.69	7288.72	3895.40	419.86
30	2.688×10^3	3372.35	7744.53	3808.73	423.56
40	2.898×10^3	3151.89	7987.80	3571.81	407.29
50	3.086×10^3	2886.38	8146.42	3279.92	381.92
60	3.260×10^3	2656.17	8420.52	3024.84	358.71

(Note: ρ is density, V_s transverse sound velocity, V_l longitudinal sound velocity, V_m average sound velocity, Θ_D Debye temperature.)

As in Tab.III a), it is found that the total charge transfer from Ca atoms to Mg atoms at 0*GPa* is 3.60, which shows a good agreement with the data reported in [20]. The charge transfer from Ca atoms to Mg atoms demonstrates the ionic bonding in $CaMg_2$ crystal. It is found that the charge transfer from Ca atoms to Mg atoms decreases with the increasing pressure (2.80 at 30GPa and 2.08 at 60GPa), implying that the ionic bonding is getting weaker [14] under the higher pressure.

However, the change of charge transfer in $CaMg_2$ phase is contrary to that in $MgZn_2$ and $MgCu_2$ phases reported by Liu et al. [35, 37]. This difference may be attributed to the different elements which make up $CaMg_2$, $MgCu_2$ and $MgZn_2$ phases, as Ca is alkali-earth element while Cu and Zn are not. The results here can be severed as a prediction for Laves phase made up of alkali-earth elements.

Tab.III b) has listed the calculated V_s, V_l, V_m and Θ_D from 0～60GPa of $CaMg_2$. The obtained Debye temperature of $CaMg_2$ at 0 K and 0GPa is 348.70 K, which is in agreement with the available value 327.44K[38]. It is clear that the Debye temperature increases under 0～30*GPa* with increasingly applied pressure then presents a declining trend when the applied pressure is above 30*GPa*.

Unfortunately, it is difficult to make comparisons with available experimental values as there is no experimental result under high pressure of $CaMg_2$ phase reported. Thus the current results can act as a theoretical prediction for future experiments.

IV. Conclusions

Structural, elastic and electronic properties of $CaMg_2$ Laves phase under external pressure from 0～60*GPa* are investigated by DFT. Conclusions are as follows:

1) The optimized structural parameters (*a*=*b*=6.250Å, *c*=10.101Å, *V*=341.732 Å^3) are very close to experimental values. From DFT calculation, $CaMg_2$ Laves phase under 0～60GPa does not undergo a phase transition, and the compressibility in *a* direction is better than in *c* direction.

2) Based on the five independent elastic constants calculated by DFT, the mechanical parameters of $CaMg_2$ at the pressure of 0*GPa* are derived as: bulk modulus is 29.659*GPa*, shear modulus 18.553*GPa*, Young's modulus 49.286*GPa*, Poisson's ratio 0.196 and elastic anisotropy factor 1.11. The results show that the applied pressure is beneficial to elastic properties. Moreover, the ductility of $CaMg_2$ is discussed in terms of the *G/B* ratio of shear modulus to bulk modulus. The calculated *G/B* ratio at 0GPa 0.663 is higher than the critical value 0.57, which indicates slight brittleness of $CaMg_2$ phase at zero pressure. The *G/B* ratio shows a decreasing tendency with the increase of pressure. As the pressure above 4GPa, the *G/B* ratio decreases with the increasing pressure, implying the good ductility of $CaMg_2$ under pressure.

3) From DOS analysis at 0, 20, 40 and 60*GPa* show that below Fermi level the total DOS is mainly made up of Mg *s*, *p* orbits while above Fermi level Ca *s*, *p* orbits contribute much to the total DOS. Moreover, the DOS reveals the existence of covalent bonding in the $CaMg_2$ crystal according to the orbital hybridization of Mg *s*, *p* and Ca *s*, *p* orbits.

The Mulliken electronic population demonstrates the charge transfer from Ca atoms to Mg atoms becomes less with the increase of pressure, which indicates the ionic bond between Ca atoms and Mg atoms becomes weaker.

4) The Debye temperature shows an increasing tendency with the applied pressure from 0 ～30GPa and then presents a declining tendency under the pressure region of 30GPa～60GPa.

V. Acknowledgment

The authors greatly acknowledge the financial support for this work provided by China Scholarship Council (CSC) and some support of state key laboratory of solidification processing, Northwestern Polytechnical University.

VI. References

[1] C. Potzies, K.U. Kainer, "Fatigue of magnesium alloys." *Advanced Engineering Materials*, vol.6, pp.281-289, 2004.

[2] Z.B. Sajuri, T. Umehara,Y. Miyashita et al., "Fatigue‐Life Prediction of Magnesium Alloys for Structural Applications," *Advanced engineering materials*, vol.5, pp. 910-916, 2003.

[3] B.Y. Tang, W.Y.Yu, X.Q. Zeng et al., "First-principles study of the electronic structure and mechanical properties of CaMg 2 Laves phase." *Materials Science and Engineering: A*, vol.489, pp. 444-450, 2008.

[4] B.L. Mordike, T. Ebert, "Magnesium: properties-applications-potential." *Materials Science and Engineering: A*, vol.302, pp. 37-45, 2001.

[5] K. Oh-Ishi, C.L. Mendis, T. Homma, S. Kamado et al., "Bimodally grained microstructure development during hot extrusion of Mg–2.4Zn–0.1Ag–0.1Ca–0.16Zr(at.%) alloys." *Acta Materialia*, vol.57, pp.5593-5604, 2009.

[6] Y. Tsushio, E. Akiba. "Hydrogenation properties of Mg-based Laves phase alloys." *Journal of alloys and compounds*, vol.269, pp.219-223, 1998.

[7] N. Hanada, S. Orimo, H. Fujii, "Hydriding properties of ordered-/disordered-Mg-based ternary Laves phase structures." *Journal of alloys and compounds*, vol.356, pp.429-432, 2003.

[8] G. Yuan, Y. Liu, W. Ding, et al. "Effects of extrusion on the microstructure and mechanical properties of Mg–Zn–Gd alloy reinforced with quasicrystalline particles." *Materials Science and Engineering: A*, vol.474, pp.348-354, 2008.

[9] Y. Liu, G. Yuan, W. Ding, et al. "Deformation behavior of Mg–Zn–Gd-based alloys reinforced with quasicrystal and Laves phases at elevated temperatures." *Journal of alloys and compounds*, vol.427, pp.160-165, 2007.

[10] N. Terashita, K. Kobayashi, T. Sasai, et al. "Structural and hydriding properties of (Mg 1− x Ca x) Ni 2 Laves phase alloys." *Journal of alloys and compounds*, vol.327, pp.275-280, 2001.

[11] H. Yamada, H. Shimizu, "Magnetic states of MgCo 2 and CaCo 2 with the cubic and hexagonal Laves phase structures." Journal of alloys and compounds, vol.388, pp.15-18, 2005.

[12] W. Chen, J.Sun, "The electronic structure and mechanical properties of MgCu 2 Laves phase compound." Physica B: Condensed Matter, 2006, 382(1): 279-284.

[13] A. Suzuki, N. D. Saddock, J. W. Jones, et al. "Structure and transition of eutectic (Mg, Al) 2 Ca Laves phase in a die-cast Mg–Al–Ca base alloy." *Scripta Materialia*, vol.51, pp.1005-1010, 2004.

[14] A. Suzuki, N.D. Saddock, J.W. Jones, T.M. Pollock, "Solidification paths and eutectic intermetallic phases in Mg–Al–Ca ternary alloys." *Acta Materialia*, vol.53, pp.2823-2834, 2005.

[15] J. F. Nie, "Preface to viewpoint set on: phase transformations and deformation in magnesium alloys." *Scripta Materialia*, vol.48, pp.981-984, 2003.

[16] J.F. Fan, G.C. Yang et al., "Oxidation behavior of ignition-proof magnesium-calcium alloys [J]." *The Chinese Journal of Nonferrous Metals*, vol.10, pp.008, 2004.

[17] P. Zhou and H. R. Gong, "Phase stability, mechanical property, and electronic structure of an Mg–Ca system." *Journal of the mechanical behavior of biomedical materials*, vol.8, pp.154-164, 2012.

[18] K. Aono, S. Orimo, and H. Fujii. "Structural and hydriding properties of MgYNi4: A new intermetallic compound with C15b-type Laves phase structure." *Journal of alloys and compounds*, vol.309, pp.L1-L4, 2000.

[19] W.Y. Yu, N. Wang, X.B. Xiao, B.Y. Tang et al., "First-principles investigation of the binary AB2 type Laves phase in Mg–Al–Ca alloy: Electronic structure and elastic properties." *Solid State Sciences*, vol.11, pp.1400-1407, 2009.

[20] Mao P, Yu B, Liu Z, et al. "First-principles calculations of structural, elastic and electronic properties of AB 2 type intermetallics in Mg–Zn–Ca–Cu alloy." *Journal of Magnesium and Alloys*, vol.1, pp.256-262, 2013.

[21] A. Aaeid, PhD Thesis, "Études ab initio et dynamique moléculaire des propriétés structurales et thermodynamiques de la calcite et la witherite sous hautes pressions", l'Université des Sciences et Technologies de Lille, 2010 France. (French)

[22] Wu Z, Zhao E, Xiang H, et al., "Crystal structures and elastic properties of superhard IrN2 and IrN3 from first principles." *Physical Review B*, vol.76, pp. 054115, 2007.

[23] F. Jia, B. Fabrice., K-B. Siham, "First-principles calculations of typical anisotropic cubic and hexagonal structures and homogenized moduli estimation based on the Y- parameter: Application to CaO, MgO, CH and Calcite CaCO3", *Journal of Physics and Chemistry of Solids*, vol.101, pp.74-89, 2017.

[24] F. Jia, B. Fabrice., K-B. Siham, "Multiscale Modeling and Mechanical Properties of Zigzag CNT and Triple-Layer Graphene Sheet Based on Atomic Finite Element Method", *Journal of Nano Research*, vol.33, pp.92-105, 2015.

[25] R. Hill, "The elastic behaviour of a crystalline aggregate" *Proceedings of the Physical Society. Section A*, vol.65, pp.349, 1952.

[26] O.L.Anderson, "A simplified method for calculating the Debye temperature from elastic constants." *Journal of Physics and Chemistry of Solids* , vol.24, pp.909-917, 1963.

[27] W. Kohn, L. Sham, "Self-consistent equations including exchange and correlation effects", *Physical review*, vol.140, pp.A1133, 1965.

[28] J. P. Perdew, K. Burke, M. Ernzerhof, "Generalized gradient approximation made simple." *Physical review letters*, vol.77, pp.3865, 1996.

[29] F. Birch, "Finite strain isotherm and velocities for single‐crystal and polycrystalline NaCl at high pressures and 300° K." *Journal of Geophysical Research: Solid Earth*, vol.83, pp.1257-1268, 1978.

[30] F. D. Murnaghan, "The compressibility of media under extreme pressures."*Proceedings of the National Academy of Sciences*, vol.30, pp.244-247, 1944.

[31] H. J. Monkhorst, J. D.Pack, "Special points for Brillouin-zone integrations." *Physical review B*, vol.13, pp.5188, 1976.

[32] T. H. Fischer, J. Almlof, "General methods for geometry and wave function optimization." *The Journal of Physical Chemistry*, vol.96, pp.9768-9774, 1992.

[33] J. Feng, B. Xiao, R. Zhou, et al. "Anisotropic elastic and thermal properties of the double perovskite slab–rock salt layer Ln2SrAl2O7 (Ln= La, Nd, Sm, Eu, Gd or Dy) natural superlattice structure." *Acta Materialia*, vol.60, pp.3380-3392 2012.

[34] V. Milman, M. C. Warren, "Elasticity of hexagonal BeO." *Journal of Physics: Condensed Matter*, vol.13, pp.241, 2001.

[35] Y. Liu, W.C. Hu, D.J. Li, X.Q. Zeng, C.S. Xu, X.J. Yang, "Structural, electronic and thermodynamic properties of BiF 3-type Mg 3 Gd compound: A first-principle study." *Physica B: Condensed Matter*, vol.432, pp.33-39, 2014.
[36] S.F. Pugh, "XCII. Relations between the elastic moduli and the plastic properties of polycrystalline pure metals." *The London, Edinburgh, and Dublin Philosophical Magazine and Journal of Science,* vol.45, pp.823-843, 1954.
[37] Y. Liu, W.C. Hu, D. Li, et al. "First-principles investigation of structural and electronic properties of MgCu 2 Laves phase under pressure." *Intermetallics*, vol.31, pp.257-263, 2012.
[38] P.L. Mao, B. Yu, Z. Liu, F. Wang, Y. Ju, "Mechanical, electronic and thermodynamic properties of Mg 2 Ca Laves phase under high pressure: a first-principles calculation." *Computational Materials Science*, vol.88, pp.61-70, 2014.

FU Jia, male, doctor degree in INSA de Rennes in France, as a visting scholar in the department of Material & Chemistry in Southern University of Science and technology, China. His research topics are focused on: Multi-scale modeling and properties calculation; Elastic-plastic behavior of the new innovative material; Thermal deformation and microstructure evolution; Nano-crystal anisotropy and homogenization; Metal plastic forming simulation. Papers published more than 15.

Lin Weihui, phd student, holds a full time position in Taiyuan University of Technology. He has been working in the Material Research program in since 2014. His research topics are focused on: Mechanical properties of the new alloy materials, Atomic Simulation of Graphene - Polymer Composites.

CHEN Zhongren, doctor degree in California Institute of Technology (Caltech), a lecture professor in the department of material chemistry in Southern University of Science and Technology. He has close cooperation with his doctoral tutors (the 2005 Nobel Price winner Robert H. Grubbs and professor Julia Ann Kornfield in Caltech) and awarded many competitive scientist medals. His research is in the area of molecular design and simulation of new material, multi-scale processing of micro/nano materials, catalysis, nanostructure characterization and polymer nanomaterials. He is on the reviewing board of the editorial advisory board of many international journals. He has published over 60 papers, including the published article in the journal of Science.